JGR Oceans

Key Points:

- Freshwater input has significantly contributed to the surface warming at the peak of the 1995 Benguela Niño
- Anomalously high river discharge and precipitation increased stratification and reduced turbulent heat loss by creating barrier layers
- Combination of high freshwater input and strong poleward surface current might play a role in temperature variability off Angola

Author Contributions:

Conceptualization: L. C. Aroucha, J. F. Lübbecke
Data curation: L. C. Aroucha, J. F. Lübbecke, M. Körner, R. A. Imbol Koungue
Formal analysis: L. C. Aroucha, J. F. Lübbecke, M. Körner, R. A. Imbol Koungue, F. M. Awo
Funding acquisition: L. C. Aroucha, M. Körner, R. A. Imbol Koungue
Investigation: L. C. Aroucha, J. F. Lübbecke, M. Körner, R. A. Imbol Koungue, F. M. Awo
Methodology: L. C. Aroucha, J. F. Lübbecke, M. Körner, R. A. Imbol Koungue

The Influence of Freshwater Input on the Evolution of the 1995 Benguela Niño

L. C. Aroucha[1] , **J. F. Lübbecke[1]** , **M. Körner[1]** , **R. A. Imbol Koungue[1]** , and **F. M. Awo[2]**

[1]GEOMAR Helmholtz Centre for Ocean Research Kiel, Kiel, Germany, [2]Nansen-Tutu Centre for Marine Environmental Research, Department of Oceanography, University of Cape Town, Cape Town, South Africa

Abstract Benguela Niño events are characterized by strong warm sea surface temperature (SST) anomalies off the Angolan and Namibian coasts. In 1995, the strongest event in the satellite era took place, impacting fish availability in both Angolan and Namibian waters. In this study, we use direct observations, satellite data, and reanalysis products to investigate the impact that the up-until-now unnoticed mechanism of freshwater input from Congo River discharge (CRD) and precipitation had on the evolution of the 1995 Benguela Niño. In the onset phase of the event, anomalous rainfall in November/December 1994 at around 6°S, combined with a high CRD, generated a low salinity plume. The plume was advected into the Angola-Namibia region in the following February/March 1995 by an anomalously strong poleward surface current generated by the relaxation of the southerly winds and shifts in the coastal wind stress curl. The presence of this low surface salinity anomaly of about −2 psu increased ocean stability by generating barrier layers, thereby reducing the turbulent heat loss, since turbulent mixing acted on a weak vertical temperature gradient. A mixed layer heat budget analysis demonstrates that southward advection of Angolan waters drove the warming at the onset, while reduced mixing played the main role at the event's peak. We conclude that a freshwater input contributed to the SST increase in this exceptionally strong event and suggest that this input can influence the SST variability in Angola-Namibia waters through a combination of high CRD, precipitation, and the presence of a strong poleward surface current.

Plain Language Summary Benguela Niño events are characterized by excessive warming of the sea surface temperature off the Angolan and Namibian coasts. One of the strongest-ever recorded warm events dates back to 1995, impacting fish availability in both Angolan and Namibian waters. In our research, we investigate if freshwater from rain and from the Congo River could have impacted the evolution of this 1995 Benguela Niño. In the event's early stage, high precipitation and river discharge generated a low salinity pool at the Congo River mouth, which in February/March 1995 was taken to the south by an exceptionally strong surface current, generated by changes in wind strength and direction at the African coast. This low sea surface salinity in a shallow layer in the upper meters of the ocean increased the ocean's stability. As the stabilized waters diminished the usual mixing from the depths below which cools down the surface waters, it contributed to an increase in warming in the surface layer of the ocean. We conclude that the warming of the surface waters in the region was indeed influenced by the combination of high precipitation and high Congo River discharge with a strong surface current toward the south.

1. Introduction

Benguela Niños are El Niño-like events in the southeastern tropical Atlantic Ocean (Figure 1) characterized by strong warm anomalies, particularly off the Angolan coast (Shannon et al., 1986; Florenchie et al., 2004). These events modulate the sea surface temperature (SST) at interannual time scales in this region and usually peak in boreal spring, from March to May, when the SSTs in the region are climatologically high (Brandt et al., 2023; Imbol Koungue et al., 2019; Lübbecke et al., 2010). At the same time, the Angola-Benguela front, that is, a thermal front located usually at 17°S due to the confluence of northern tropical warm waters and southern colder waters from the Benguela Current, is located furthest south (Lübbecke et al., 2010). During the strong warm event, positive SST anomalies can reach up to 3°C in the Angola Benguela area (ABA, here defined as 8°S–20°S, 8°E to the coast, Figure 1) consequently impacting the biology and ocean-atmosphere processes at the southwestern African coast. In fact, it has been shown that these events not only influence marine ecosystems and fisheries in the region (Binet et al., 2001; Blamey et al., 2015; Boyer & Hampton, 2001; Gammelsrød et al., 1998), modulating the upward supply of nutrients (Bachèlery et al., 2016a) but have also consequences for rainfall and

Project Administration: J. F. Lübbecke
Resources: L. C. Aroucha, J. F. Lübbecke
Software: L. C. Aroucha
Supervision: J. F. Lübbecke
Validation: L. C. Aroucha, R. A. Imbol Koungue
Visualization: L. C. Aroucha, J. F. Lübbecke, M. Körner, F. M. Awo
Writing – original draft: L. C. Aroucha
Writing – review & editing: L. C. Aroucha, J. F. Lübbecke, M. Körner, R. A. Imbol Koungue, F. M. Awo

flooding in coastal Africa (Hansingo & Reason, 2009; Lutz et al., 2015; Rouault et al., 2003). Hence, understanding the development of these warm events is of great socioeconomic importance for local communities.

Benguela Niños have been shown to be triggered mainly remotely. The relaxation of the trade winds in the western equatorial Atlantic generates eastward propagating downwelling equatorial Kelvin waves followed by coastally trapped waves (CTWs) propagating southward when reaching the African coast (Bachèlery et al., 2016b; Florenchie et al., 2004; Imbol Kounge et al., 2017; Lübbecke et al., 2010; Rouault et al., 2018). The propagation of these CTWs is also responsible for controlling the variability and seasonality of the Angola Current (Bachèlery et al., 2016b; Kopte et al., 2017). The Angola Current is a geostrophic poleward undercurrent usually situated below the equatorward coastal jet (Fennel et al., 2012; Tchipalanga, Dengler, et al., 2018), restricted to the upper 120 m of the water column and with its core at around 50 m depth (Kopte et al., 2017; Tchipalanga, Dengler, et al., 2018). This poleward current is situated closer to the sea surface seaward of the coastal jet (Fennel et al., 2012). The passage of a downwelling (upwelling) CTW in austral summer (winter) enhances (weakens) the Angola current (Tchipalanga, Dengler, et al., 2018), with the downwelling waves deepening the thermocline, resulting in a high SST anomaly. Bachèlery et al. (2020) showed that 71% of both Benguela Niños and Niñas (i.e., the counterpart of Benguela Niño events, where SST is anomalously cold in ABA) events are forced remotely at the equator.

Local forcing, however, also plays an important role in generating and modulating these coastal warm anomalies due to local wind fluctuations (Hu & Huang, 2007; Illig et al., 2020; Polo et al., 2008) in association with shifts in the position and strength of the South Atlantic Anticyclone (Richter et al., 2010) by modulating upwelling intensity and consequently SST at western coastal Africa. In addition, local wind forcing plays a major role in determining the structure and variability of the eastern boundary circulation in this area (Fennel et al., 2012; Junker et al., 2015), which are usually impacted by the southerly winds related to the atmospheric Benguela low-level coastal jet (Patricola & Chang, 2017). Imbol Koungue et al. (2021) showed that a combination of both local and remote forcing was important in triggering the 2019 Benguela Niño, and Lübbecke et al. (2019) suggested that local wind forcing in combination with anomalous high freshwater input into the ocean due to both local precipitation and Congo River discharge (CRD) impacted the generation of the 2016 warm event in the southeastern tropical Atlantic.

The role of freshwater input in the development of warm events is through the generation of barrier layers (Figures 1b and 1c). The presence of barrier layers increases ocean stability and stratification, hence reducing the mixing and entrainment of cool subsurface waters into the mixed layer, thereby leading to an SST increase. In fact, in the Pacific, it has long been shown that freshwater input can impact surface warming by the generation of these barrier layers associated with a decrease in entrainment cooling (Vialard & Delecluse, 1998). For the eastern tropical Atlantic, Materia et al. (2012) showed the effect of Congo River freshwater discharge on warm events occurring in the Gulf of Guinea, while White and Toumi (2014) quantified the formation of barrier layer up to 6 m thick in model simulations due to an mixed layer shoaling by the CRD. However, the role of freshwater input for SST variability in the southeastern tropical Atlantic has not been fully elucidated by modeling studies (White & Toumi, 2014). More recently, Sena Martins and Stammer (2022), despite not being able to find a significant correlation between the river plume patterns and the occurrence of a Benguela Niño, showed evidence for a strong influence of the CRD low-salinity layer in increasing stratification in the region.

The 1995 Benguela Niño was the strongest event ever recorded in the satellite era (Imbol Koungue et al., 2019) evidencing SST anomalies averaged for February-March-April up to 3°C in the region (Figure 1a). It was first described by Gammelsrød et al. (1998) and was associated with high mortality and southward displacement of fish from Angolan to Namibian waters, also economically impacting these countries. The eastward propagation of an equatorial Kelvin wave followed by a southward CTW along the African coast was shown through forced ocean simulations at the onset of the event (Imbol Koungue et al., 2019), and was associated with a 0.73°C increase in the peak of SST anomalies (Imbol Koungue & Brandt, 2021). On the other hand, no clear evidence of a Kelvin wave influence was detected from satellite observations, with the sea surface height anomalies appearing to be stationary and not propagating along the southwestern African coast (Richter et al., 2010). In fact, the role of remote forcing via the propagation of a Kelvin wave was not the most pronounced in the 1995 Benguela Niño in comparison with other warm event years (e.g., 1984, 2010/2011; see Figure 6 from Imbol Koungue et al., 2019). More recently, Song et al. (2023) when simulating Benguela Niño/Niña events with a single-layer ocean linear model excluding the local forcings (e.g., precipitation and freshwater advection) did not find a clear energy route
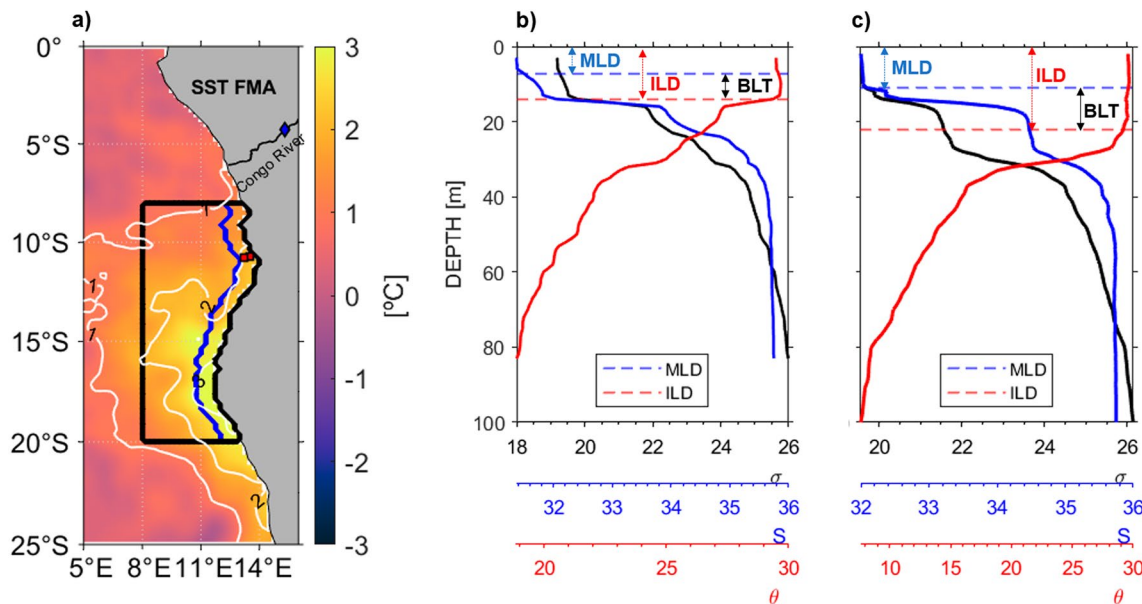
Figure 1. (a) Detrended monthly sea surface temperature (SST) anomalies from NOAA Optimum Interpolation SST for February-March-April 1995. White contours are anomaly isotherms 1°C apart from each other. Blue diamond represents Congo River Brazzaville station. Contours indicate ABA (8°S–20°S, 8°E to the coast, black) and coastal box 1 (8°S–20°S, 1° away from the coast, blue). Red squares indicate the location of conductivity-temperature-depth (CTD) profiles depicted in (b), (c). CTD profiles from Nansen Program (b) on 16 March 1995 at 10.74°S and 13.5°E and (c) on 27 March 1995 at 10.76°S and 13.2°E. Red, blue, and black solid lines in (b)**,** (c) represent potential temperature (θ), salinity (S), and density (σ) profiles, respectively. MLD, mixed layer depth; ILD, isothermal layer depth; BLT, barrier layer thickness.

of equatorial waves (i.e., remote forcing) triggering the 1995 extreme warm event. The authors suggested that the coastal SST anomaly might have been forced locally for this year (Song et al., 2023). Finally, in Gammelsrød et al. (1998), Conductivity-Temperature-Depth (CTD) profiles identified the presence of a freshwater plume of low salinity at 18°S in March 1995, much further south than climatologically expected (i.e., maximum southward displacement extending only to around 12°S in February-March-April; Awo et al., 2022). At the same time, similar CTD profiles showed the occurrence of barrier layers at 9°S (see Figure 2b from Gammelsrød et al., 1998). Although Gammelsrød et al. (1998) associated the Benguela Niño event with these strong negative salinity anomalies on the Angolan coast, the study did not mention the barrier layers presence or possible impacts on this event. Overall, it seems that both remote and local forcing played a role in the generation of this event.

The aim of this paper is to evaluate the impact of the high freshwater input followed by the strong low salinity signal in the 1995 Benguela Niño event. We intend to depict and discuss an up-until-now unnoticed effect of the increased stratification through the presence of barrier layers in the strongest warm event ever recorded in the southeastern tropical Atlantic. We also use a mixed layer heat budget analysis to discuss the oceanic and atmospheric processes responsible for the high SST signal. For that, we use satellite data and reanalysis products, comparing them to diverse in-situ measurements, including CTD profiles and sections from different cruises, and a mooring situated in the region. The paper is divided as follows: in Section 2 we introduce the different data sets used and the methods for defining the barrier layer and the mixed layer heat budget terms. In Section 3 we describe not only the processes that led to a high freshwater input in the ABA at the onset of the event, and the impacts of this input on the water column stratification, but also the different processes related to the heat budget terms that were responsible for the warming during the event. In Section 4, we discuss the results and future perspectives, and end with concluding remarks.

2. Data and Methods

2.1. Data Sets

SST monthly averages were obtained from the high-resolution NOAA Optimum Interpolation SST (OISST), with 0.25° spatial resolution, which consists of a blend of satellite and in-situ measurements (Huang et al., 2021;

Reynolds et al., 2007). OISST data is available at National Centers for Environmental Information (www.ncei. noaa.gov) from 1981 to the present day.

We use monthly averages of the 6-hourly wind vectors from the Cross-Calibrated Multi-Platform (CCMP) (Atlas et al., 2011; Mears et al., 2022). CCMP combines a background field from European Center for Medium-Range Weather Forecasts (ECMWF) reanalysis 5 (ERA5, Hersbach et al., 2020) with 10-m wind retrievals over the ocean from different types of satellites. CCMP data is available from 1993 to 2019, with a $0.25° \times 0.25°$ spatial resolution, at the Remote Sensing Systems platform (www.remss.com). We calculate wind stress by applying the bulk formula $\vec{\tau} = \rho_a \ x \ c_D \ x \ \overrightarrow{u_{10}} \ x \ u_{10}$, with $\rho_a = 1.22$ kg m^{-3} and $c_D = 0.0013$.

Monthly surface heat fluxes, that is, Shortwave Radiation (SWR), Longwave Radiation (LWR), Latent Heat Flux (LHF), and Sensible Heat Flux (SHF) were used from the ERA5 reanalysis (Hersbach et al., 2020). This data is available at 0.25° horizontal resolution from 1940 to present days and is distributed by the Copernicus Climate Change Service via https://cds.climate.copernicus.eu/.

Furthermore, for the freshwater input data, monthly Congo River discharge measurements were obtained from SO-HYBAM (http://www.ore-hybam.org/) at Brazzaville Station, Republic of Congo, available from 1947 to 2019. Monthly means of precipitation from merged satellite and surface rain gauge observations, with $2.5° \times 2.5°$ spatial resolution, were taken from the Global Precipitation Climatology Project (GPCP) (Adler et al., 2003). Data is accessible from 1979 to 2020 at https://psl.noaa.gov.

Finally, monthly means of potential temperature, salinity, zonal and meridional currents from the Global Mercator Ocean Reanalysis product (GLORYS12) (Lellouche et al., 2021) were used in order to calculate the Mixed Layer Depth (MLD), Isothermal Layer Depth (ILD), and consequently Barrier Layer Thickness (BLT). The Brunt-Väisälä frequency (N^2) calculations were also based on this product as well as the Mixed Layer Heat Budget analysis described in Section 2.2.2. The product has a 1/12° spatial resolution and 50 vertical levels, with 1m vertical resolution in the first levels, increasing with depth, and data available from 1993–2019. This data set is distributed by the EU Copernicus Marine Service Information (http://marine.copernicus.eu/).

Since GLORYS12 and CCMP products are limited to the time period 1993–2019, only these 27 years were used for all above-cited data sets. Detrended anomalies for each data set were calculated by removing within the same period monthly climatologies and trends from the data. In order to evaluate how well GLORYS12 represents the main processes occurring in ABA, in-situ measurements were compared to this reanalysis product. The assessment and validation of the GLORYS12 product against in-situ measurements are provided in Text S1 in Supporting Information S1. Text S1 in Supporting Information S1 also describes the observational data sets used to perform this analysis.

2.2. Methods

2.2.1. Barrier Layer Thickness

In this study, we define the Mixed Layer Depth (MLD) as the depth at which potential density (σ_Θ) is increased by $\Delta\sigma_\Theta$ relative to its own value at a reference depth, as follows (de Boyer Montégut et al., 2004, 2007; Gévaudan et al., 2021; Mignot et al., 2012; Saha et al., 2021; White & Toumi, 2014):

$$\text{MLD}: depth \, where \, \sigma_\Theta = \sigma_{\text{rfd}} + \Delta\sigma_\Theta \tag{1}$$

$$\Delta\sigma_\Theta = \sigma_\Theta(T_{\text{rfd}} - 0.2°C, S_{\text{rfd}}, P_0) - \sigma_\Theta(T_{\text{rfd}}, S_{\text{rfd}}, P_0) \tag{2}$$

where *rfd* represents the surface level of the GLORYS12 reanalysis (i.e., ∼0.5 m) as the reference depth. $\Delta\sigma_\Theta$ represents the potential density change equivalent to a 0.2°C temperature decrease at the local salinity. P_0 is the pressure at the ocean surface, and T_{rfd} and S_{rfd} are respectively the temperature and salinity at the reference depth. At the same time, the ILD is defined by a 0.2°C threshold, where:

$$\text{ILD}: depth \, where \, T = T_{\text{rfd}} - 0.2°C \tag{3}$$

Finally, the Barrier Layer Thickness (BLT) definition is the difference between the ILD and the MLD:

$$\text{BLT} = \text{ILD} - \text{MLD} \tag{4}$$

Additionally, for the identification of the stability and stratification of the water column within the 1995 event, the Brunt-Väisälä frequency N^2 was also obtained at each depth by using the same GLORYS12 product. Then, N^2 was averaged from the MLD until 50 m, since the MLD in this region is climatologically shallower than 50 m (not shown). Both anomalies of BLT and N^2 were calculated by removing the climatology within the 1993–2019 period.

2.2.2. Mixed Layer Heat Budget

In order to assess the processes driving the temperature change during the 1995 Benguela Niño, reanalysis, and satellite products were used to perform a mixed layer heat budget analysis. Here we use an approach similar to several previous papers (e.g., Echols & Riser, 2020; Foltz et al., 2003, 2020; Körner et al., 2023; Moisan & Niiler, 1998; Stevenson & Niiler, 1983). The equation used here is as follows:

$$\frac{\partial T}{\partial t} = -\boldsymbol{v} \cdot \nabla T + \frac{q_{net}}{\rho\, c_p\, h} + r \tag{5}$$

where $\partial t = 1$ month; $T = \overline{T_{ML}}$, which is the temperature averaged for the mixed layer; $\boldsymbol{v}$ represents the horizontal currents averaged for the mixed layer $h = $ MLD; ρ is the seawater density, taken here as 1025 kg/m^3; c_p is specific heat capacity taken as 4000 J/kg °C. From left to right each term denotes respectively: Mixed layer temperature tendency, temperature horizontal advection within the mixed layer, net surface flux corrected for the SWR that penetrates into the mixed layer, and residual. The residual contains the terms not represented in the equation, such as turbulent heat loss (i.e., heat loss at the base of the mixed layer due to turbulent mixing), entrainment, and the vertical temperature velocity covariance (Foltz et al., 2003; Hummels et al., 2014; Körner et al., 2023). Actually, the temperature/velocity covariance is considerably smaller than the other contributions and is usually neglected in the ML heat budget analysis (Foltz et al., 2003; Hummels et al., 2014; Körner et al., 2023). In addition, the residual includes the contribution of processes unresolved by the spatial and temporal scales of the data used here, and the uncertainty arising from the data.

The net surface heat flux term (q_{net}) consists of the sum of q_{abs}, LWR, LHF, and SHF, where q_{abs} represents the amount of shortwave radiation absorbed within the mixed layer. Here, q_{abs} is defined based on Foltz et al. (2020) where: $q_{abs} = SWR\left(1 - 0.47e^{-h/15}\right)$, considering an albedo rate of 6% where h is the MLD in meters. All heat fluxes used here were obtained from the ERA5 reanalysis data set and interpolated into the GLORYS12 grid.

3. Results

3.1. Low-Salinity Plume Propagation

The 1995 Benguela Niño event started to develop in February when positive SST anomalies of 2°C averaged for the ABA coastal region (i.e. coastal box 1) were observed (Figures 2a and 3a). The event peaked 1 month later, in March, when the ocean surface temperature was up to at least 4°C warmer than climatology close to the Angola-Benguela front (Figure 2a). One characteristic of this event was that the positive SST anomalies were not restricted to the ABA, but reached south of 20°S extending also to the northern Namibian upwelling region around 23°S (Figure 2a, also Gammelsrød et al., 1998). In fact, a similar pattern was observed during the 2010/2011 Benguela Niño event, when the strong poleward subsurface Angola current advected warm waters as far as 25°S (Rouault et al., 2018). In April, warmer waters remained in the region until the demise of the event in May. Concurrently, at the onset of the event in February 1995, a low-salinity plume with negative sea surface salinity (SSS) anomalies of up to −3 psu was present in the area, apparently advected poleward from the north (Figure 2b). This poleward propagation of the low-salinity is consistent with the local current speed and will be addressed in Section 3.2. At the peak of the event in March 1995, this freshwater plume was observed at around 18°S, much further south than climatologically expected. In February and March, low-salinity waters in the region, mainly generated by the outflow of the Congo River (blue diamond in Figure 2), are expected to have their maximum southward extension until 12°S (Awo et al., 2022). The mean observed SSS anomaly for the coastal box 1(8°S–20°S, 1° wide band along the coast) was almost −2 psu at the onset of the 1995 event in February, and remained strong in March (Figure 3d). The freshwater influence was initially restricted to the coastal area off Angola, but expanded further offshore in March. In April, the low-salinity pattern started to vanish and the anomalies at the coastal box were within the limit of the standard deviation for this month (Figures 2b and 3d). Figures 3a and 3c show that both signals of low SSS and high SST anomalies from the coast to 1° degree offshore
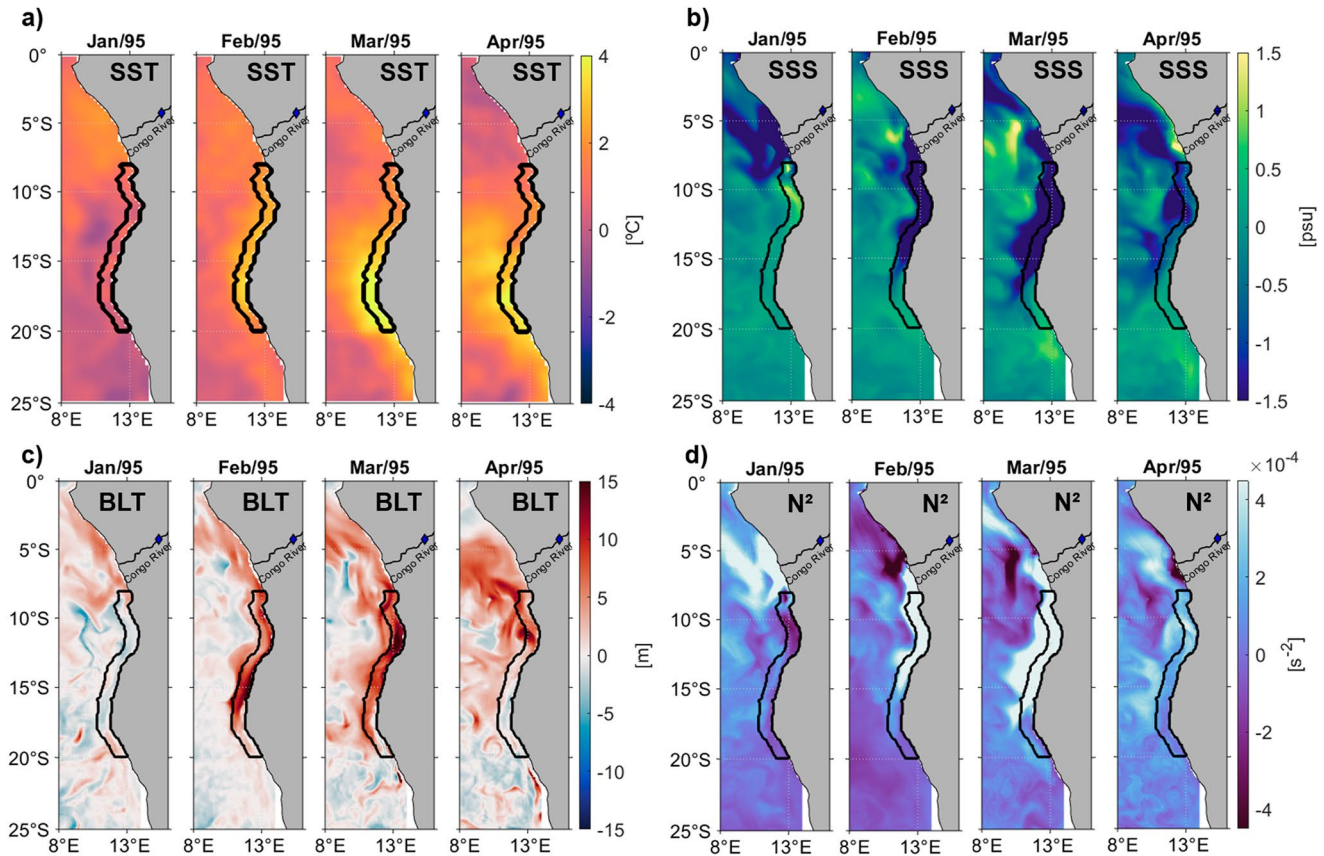
Figure 2. Detrended monthly anomalies from January–April 1995 for sea surface temperature (SST) (a), sea surface salinity (SSS) (b), Barrier Layer Thickness (BLT) (c), N^2 (d). Black contours indicate coastal box 1 region (8°S–20°S, 1° away from coast). Blue diamond represents Congo River Brazzaville station. SST from NOAA Optimum Interpolation SST. SSS from Global Mercator Ocean Reanalysis product (GLORYS12), BLT and N^2 calculated from GLORYS12 data set.

are the strongest ones detected for the analyzed period. Negative anomalies of SSS at the coast also peaked at the beginning of 2016 (Figure 3c) during the 2016 warm event. Indeed, Lübbecke et al. (2019) showed that a high freshwater input into the region might also have influenced the SST warming during this event.

Low surface salinities can lead to the formation of barrier layers and enhance the upper ocean stratification. Concomitant patterns of positive BLT and N^2 anomalies were observed close to the coast at the beginning of the event, reaching further south and spreading offshore in March (Figures 2c and 2d). BLT anomalies of up to 15 m indicate strong anomalous stratification of the water column, which is also reflected in its stability indicated by the Brünt-Väisäla frequency positive anomaly. The barrier layer presence could also be observed in the CTD profiles taken from the Nansen Program in 1995 (Figures 1b and 1c). The vertical profiles (Figures 1b and 1c) show a significant change within 10 days, which is an indication of the importance of submonthly processes acting in the region (Bachèlery et al., 2016b; Goubanova et al., 2013). However, from the vertical profiles of temperature, salinity, and density (not shown) we can see that the presence of the barrier layer on the coast of Angola is persistent from the onset (February 1995) to the demise of the event (April 1995). High stratification was likewise observed during the 2016 warm event (Figures 3e and 3g, and in Lübbecke et al., 2019). Freshwater input at the ocean surface creates a shallow mixed layer, where the most pronounced salinity and density gradients are located above the highest temperature gradient (Figures 1b and 1c). The difference between the depth of these two gradients creates a more stratified water column, isolating the surface layer from the cooling from below induced by mixing and entrainment, which can favor surface warming.

In order to understand the origin of the low salinity plume, we analyzed two possible sources of freshwater input in the region during the event. Precipitation anomalies of up to 5 mm/day were observed prior to the 1995 Benguela Niño event, in November/December 1994, in the proximities of the Congo River mouth around 5°S, north of the ABA (Figure 4a). The positive anomalies 2–3 months prior to the event were the strongest
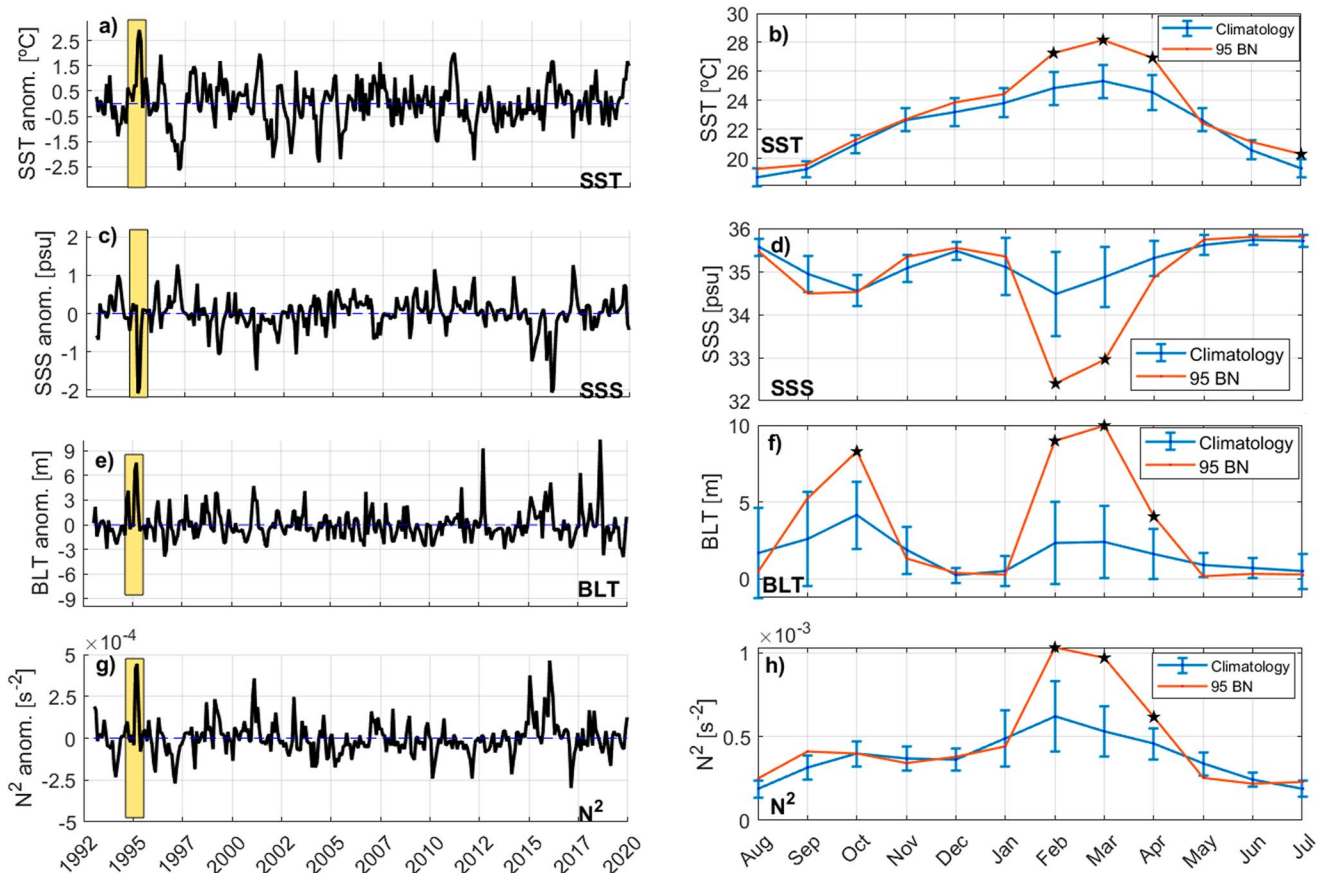
Figure 3. Detrended monthly anomalies of sea surface temperature (SST) (a), sea surface salinity (SSS) (c), Barrier Layer Thickness (BLT) (e) and N^2 (g) averaged for coastal box 1 region (8°S–20°S, 1° away from coast) from 1993 to 2019. Yellow shading indicates the period from August 1994 to July 1995. (b) SST climatology (shown from August to July, in blue) calculated over 1993–2019 and monthly values (in red) from August 1994 to July 1995 averaged in the coastal box 1. Panels (d, f, h) same as panel (b) but for SSS, BLT, and N2, respectively. Intervals in panels (b, d, f, h) depict monthly standard deviation. SST from NOAA Optimum Interpolation SST. SSS from Global Mercator Ocean Reanalysis product (GLORYS12), BLT, and N^2 calculated from GLORYS12 data set. Black stars in panels (b, d, f, and h) indicate significant differences from monthly climatologies of each respective month at a 90% confidence level according to the Student's t test.

ones recorded in the time series and were high above the monthly climatological mean and standard deviation (Figures 4b and 4c). This order of magnitude in precipitation anomalies was not seen in any other year during the 27 years analyzed period. Freshwater input averaged for the coastal box 2 region of around 3 mm/day higher than the climatology was also found in March 1995 (Figures 4a and 4c). This could already be a response to the surface warming initiated in February 1995, which brings even more non-saline water to the region via enhanced precipitation, indicating a positive feedback of freshwater input during the event. Regarding the CRD, the data indicate that only in December 1994 the river outflow was higher than climatologically expected, although the difference is not significant (Figure 4e). It also reflects the increased precipitation over land, upstream in the Congo River, from September to November/1994 (Figure 4a). The magnitude of the positive anomaly in the river discharge compared to other years was not exceptional (Figure 4d). However, one can still observe that an anomalous freshwater input from the Congo was present in December 1994, 2 months prior to the onset of the 1995 Benguela Niño.

We conclude that both anomalously high precipitation and Congo River discharge 2–3 months prior to the onset of the 1995 Benguela Niño were main contributors as freshwater sources to the event. Both sources also contributed to the 2016 warm event (Lübbecke et al., 2019). Since the stronger precipitation anomalies in 1994/1995 were located close to the Congo River mouth, one can also conclude that the anomalously high freshwater input in ABA came from the north and was advected southward. However, indicating which freshwater source was the most significant in impacting the warming is beyond the scope of this study. Overall, it was shown that due to both an above-average precipitation and CRD, a freshwater plume was generated and could propagate southward
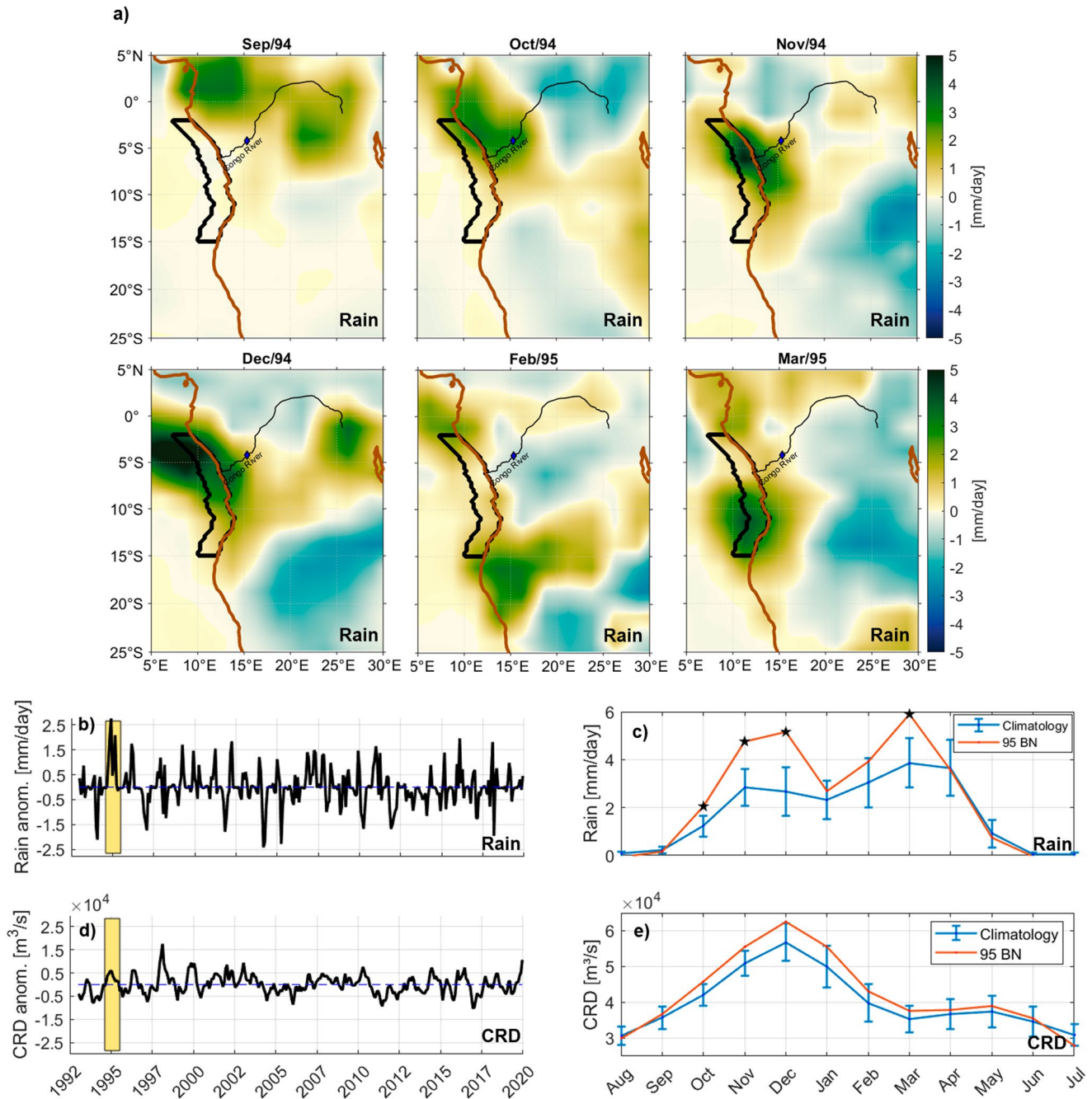
Figure 4. Detrended monthly anomalies from September 1994 to March 1995 for precipitation (a). Black thick contours indicate coastal box 2 region (2°S–15°S, 2° away from coast). Brown contour denotes coastline. Blue diamond represents Congo River Brazzaville station. Detrended monthly anomalies of precipitation averaged for coastal box 2 region (b) and Congo River discharge (d) from 1993 to 2019. Yellow shading indicates the period from August 1994 to July 1995. (c) Precipitation climatology (shown from August to July, in blue) calculated from 1993 to 2019 and monthly values (in red) from August 1994 to July 1995 averaged in the coastal box 2. Panel (e) same as panel (c) but for Congo River discharge. Intervals in Figures (c, e) depict monthly standard deviation. Black stars in panels (c) and (e) indicate significant differences from monthly climatologies of each respective month at a 90% confidence level according to the Student's *t* test.

toward the ABA, generating stability and stratification of the water column concomitant with the warm anomalies during the 1995 Benguela Niño. The processes and dynamics that allowed the southward freshwater propagation to occur will be discussed in the next section.
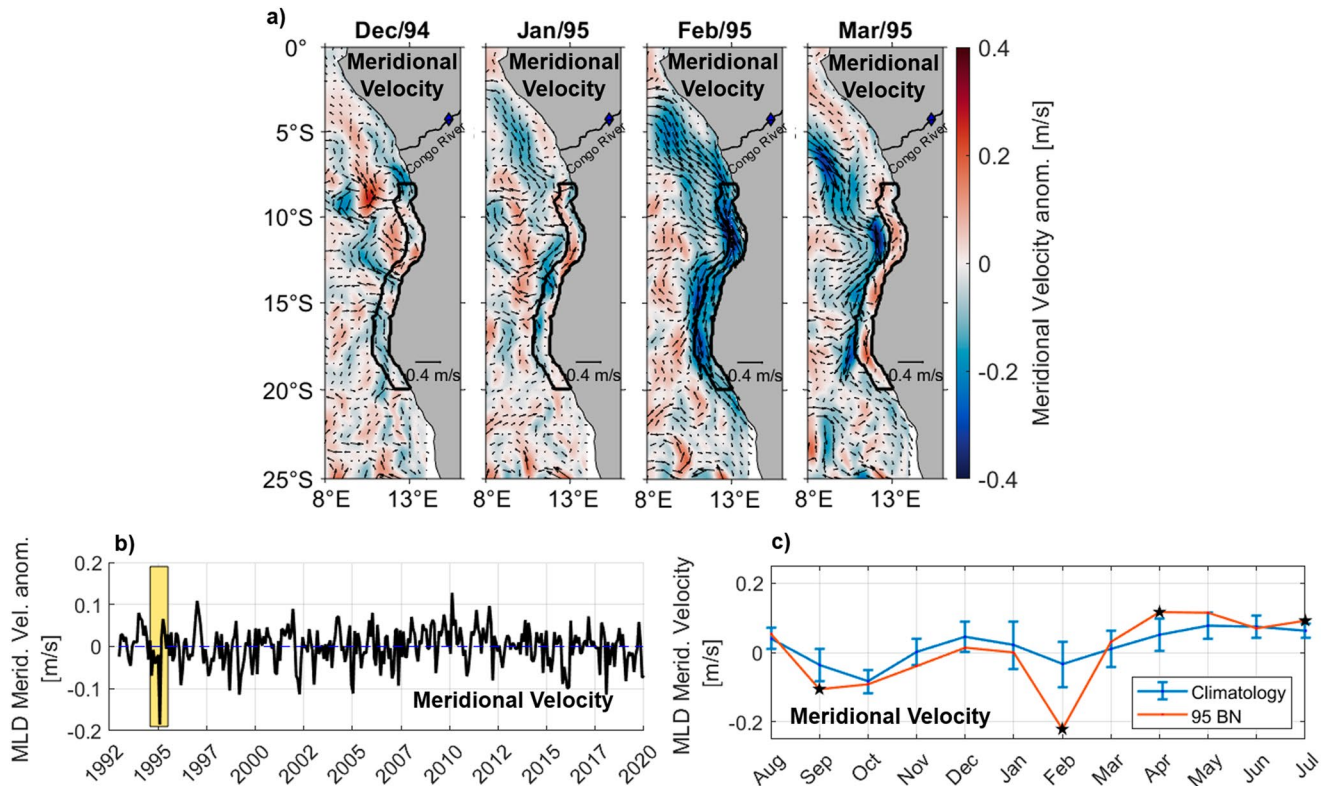
Figure 5. Detrended monthly anomalies from December 1994 to March 1995 for mixed layer meridional velocity (a). Arrows indicate the current anomaly direction. Black contours indicate coastal box 1 region. Blue diamond represents Congo River Brazzaville station. Detrended monthly anomalies of mixed layer meridional velocity averaged for coastal box 1 region from 1993 to 2019 (b). Yellow shading indicates the period from August 1994 to July 1995. Mixed layer meridional velocity climatology (shown from August to July, in blue) calculated from 1993 to 2019 and monthly values (in red) from August 1994 to July 1995 averaged in the coastal box 1 (c). Intervals in panel (c) depict monthly standard deviation. Black stars in panel (c) indicate significant differences from monthly climatologies of each respective month at a 90% confidence level according to the Student's t test.

3.2. Role of Alongshore Current and Wind Forcing

In the southeastern tropical Atlantic, low-salinity waters, mainly from the CRD, and their southward propagation are usually restricted to 12°S (Awo et al., 2022). However, as shown in the previous section, during the 1995 Benguela Niño the freshwater plume was advected further south in February and March, until around 18°S. In order to investigate what might have caused this anomalous poleward transport during the warm event, we analyzed the mixed layer meridional current anomalies from the GLORYS reanalysis product. From January 1995, a southward current anomaly at around 3°S and 2° offshore of the coast started to develop (Figure 5a). In February 1995, this negative current anomaly was even stronger (i.e., about −0.4 m/s) and was shifted closer to the coast (Figure 5a). In March 1995, the southward anomaly weakened and was again moving offshore. The really strong negative signal observed in February 1995 is even more clearly visible when averaging the current anomalies for the coastal box 1(Figures 5b and 5c). From the analyzed period, this month had by far the strongest southward current anomaly observed at the mixed layer. February 1995 was also the month with the fastest southward advection of the low salinity plume. The −1 psu signal at 10°S in January 1995 to 18°S in February 1995 (see Figure 2b) propagated southward with a roughly estimated speed of about 0.37 m/s. This estimate agrees in magnitude with the mixed layer current anomaly strength. In addition, the meridional velocity anomalies started to develop in December/January 1995 close to the Congo River mouth concomitantly with the strong precipitation observed in December in the same region.

It is known that the Angola Current has its core at subsurface (Kopte et al., 2017; Tchipalanga, Dengler, et al., 2018). It might be argued that this current could not be driving the southward transport of the low-salinity signal in the 1995 Benguela Niño, since the freshwater input generated a very shallow mixed layer and hence a surface current would be needed to carry the low-salinity plume. This raises the question of the mechanism behind the southward transport of the freshwater plume.
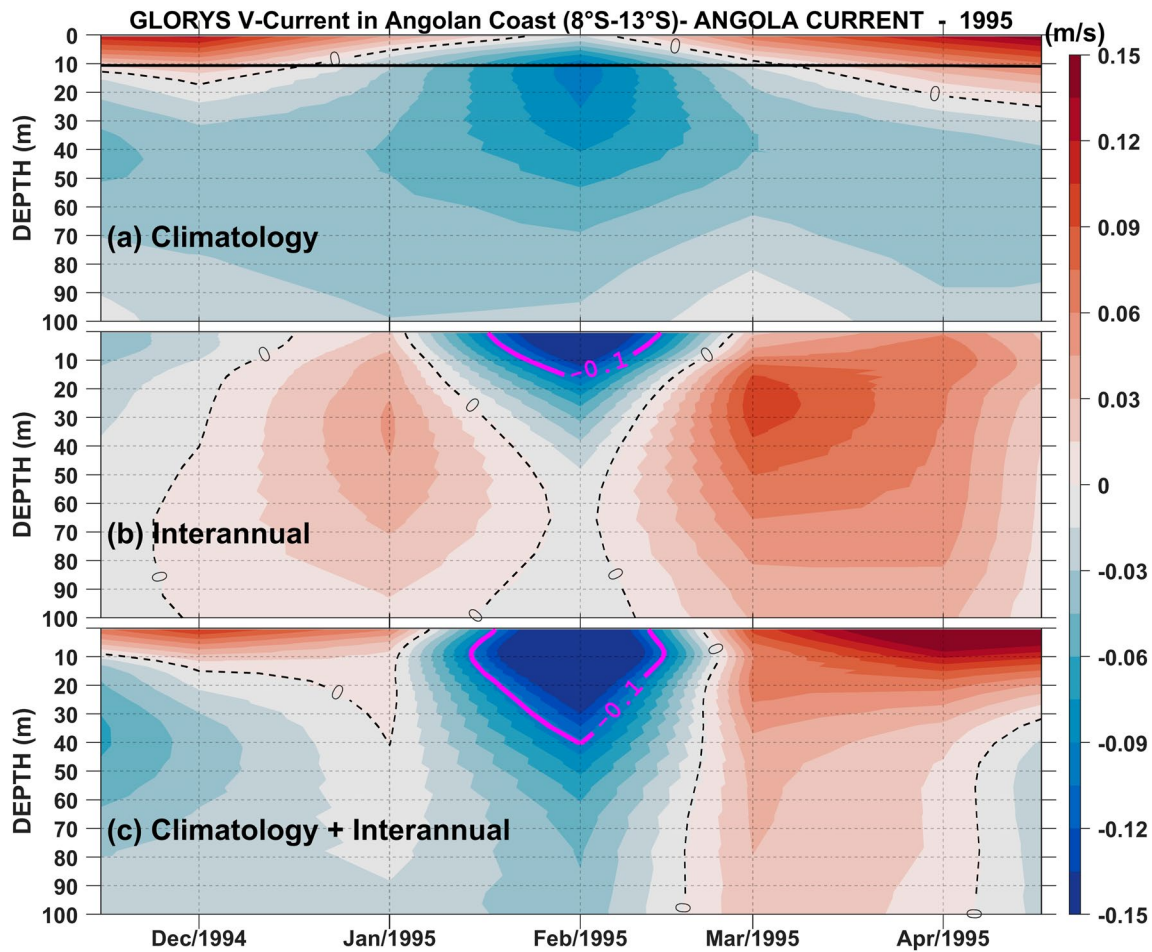
Figure 6. Depth-time Hovmöller diagram of climatology (calculated from 1993 to 2019, and shown between November and April) (a), monthly detrended anomalies (b), and absolute values (c) of coastal Angolan meridional current (*v*) averaged from 8°S to 13°S, 1° away from the coast (b, c) are shown from November 1994 to April 1995. The black line represents the density ocean mixed layer thickness obtained directly from Global Mercator Ocean Reanalysis product reanalysis, defined by sigma theta, and also averaged for the same area. Magenta contour depicts −0.1 m/s isoline.

In order to tackle this question, we analyzed both GLORYS12 velocities at depth and wind data from CCMP. From the vertical structure of the meridional current during the 1995 Benguela Niño (Figure 6), we could see an anomalously strong surface poleward current at the coast. While the Angola Current core from the GLORYS12 reanalysis is climatologically situated at 10–20m depth in February (Figure 6a), during February 1995, the strongest southward anomalies were found especially at the surface (Figure 6b). Note that during this event, not only the position of this highest poleward velocities was lifted upward but also the current strength was higher. Both of these features can only be reached by strong shifts in the wind field in the same period since local wind stress and wind stress curl are the main drivers of the strengthening and uplifting of the Angola Current (Fennel et al., 2012; Tchipalanga, Dengler, et al., 2018).

Overall, in the region, southerly winds that strengthen seaward are observed, leading to a negative (cyclonic) wind stress curl close to the coast (e.g., Lübbecke et al., 2019). However, during the 1995 event, we could observe changes in both wind stress and wind stress curl (Figure 7). From December 1994 to January 1995, the meridional wind stress weakened (Figure 7a) around 5°S–7°S, concomitant with the onset of the poleward current anomaly development (Figure 5a). In February 1995, the wind stress was even weaker offshore, and the weakening extended to the whole region, exactly at the time when the poleward current anomaly was strongest. Concomitantly, a strong weakening (strengthening) of the wind stress curl, indicated by positive (negative) anomalies in Figure 7b, was observed throughout the African coast (offshore). These shifts in the curl were most pronounced in February 1995 from 7°S to 13°S, indicating stronger than normal winds at the coast in this latitudinal band. Consequently, reduced (enhanced) coastal (offshore) wind stress curl was generated. Fennel et al. (2012) showed
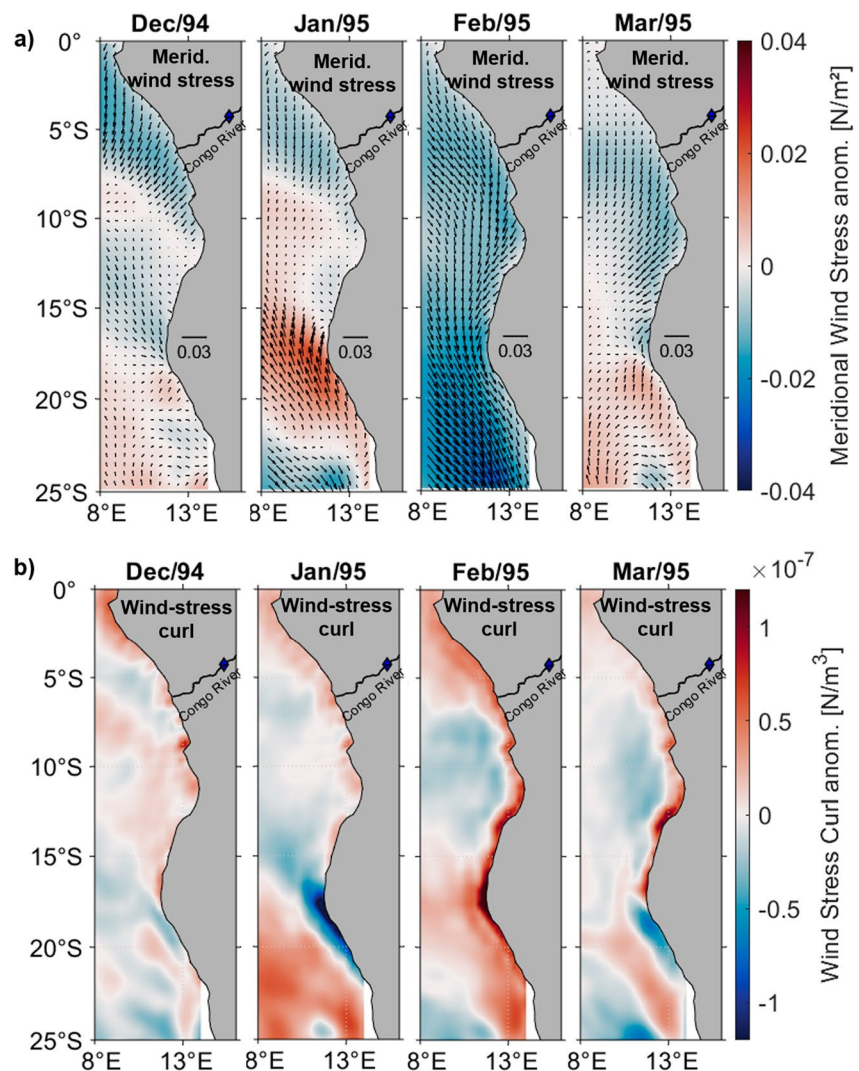
Figure 7. Detrended monthly meridional wind-stress anomalies (a) and wind-stress curl anomalies from December 1994 to March 1995 (b). Arrows indicate the direction of the wind stress anomaly. Blue diamond represents Congo River Brazzaville station. Positive values in panel (b) indicate weakening of the wind stress curl.

that under this scenario, with a diminished wind stress curl at the coast, the equatorward coastal jet weakens and the undercurrent (i.e., the Angola Current) is able to reach the surface, which explains the anomalously strong surface poleward current at the coast observed during the 1995 event.

3.3. Processes Driving the Warming

The combination of a high CRD and precipitation concomitant with the strong southward Angola Current and its uplifted core to the surface were shown to be the main drivers of the anomalous high freshwater input into the Angolan coast during the 1995 Benguela Niño. Now, we investigate what processes led to the surface warming by performing a mixed layer heat budget analysis (see Section 2.2.2) for the coastal region off Angola during this anomalous event. We first describe the mechanisms responsible for the climatological heat budget, and then discuss the anomalies during the 1995 event.

The monthly climatology of each term with its monthly standard deviation is shown in Figures 8a–8e. Figure 8f depicts the contribution of each term to the climatological surface warming (positive) and cooling (negative). As recently shown by Körner et al. (2023), the mixed layer heat content in this region is climatologically dominated by the surface heat fluxes and turbulent heat loss at the base of the mixed layer, here included in the residual

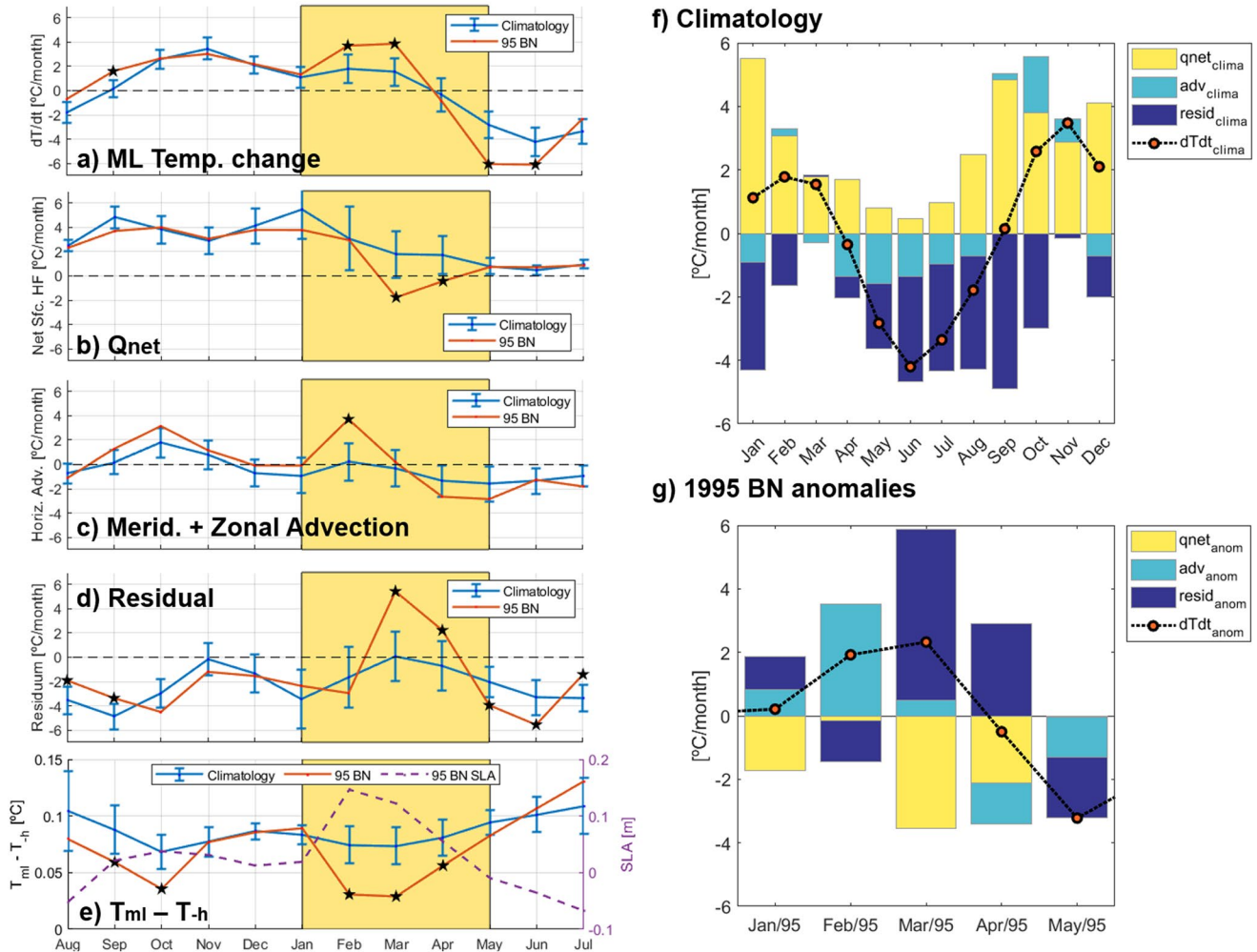**Average for coastal box 1 (8°S – 20°S, 1° off the coast)**

Figure 8. Monthly climatology (blue) of the terms from mixed layer heat budget equation averaged for coastal box 1 from 1993 to 2019 depicted from August to July for (a) temperature tendency; (b) net surface heat flux; (c) horizontal advection; (d) residual; (e) temperature gradient (i.e., difference between ML temperature and temperature at the base of ML) and Sea Level Anomaly (SLA) from GLORYS12 data set (purple dashed line). Intervals indicate monthly standard deviation. (a–e) In red are monthly values from August 1994 to July 1995 of the parameters mentioned above, respectively. (f) Climatological contribution of each calculated term for coastal box 1 mixed layer temperature between 1993 and 2019. (g) Detrended monthly anomalies of the terms from mixed layer heat budget equation averaged for coastal box 1 from November 1994 to May 1995 coastal box. Black stars in panels (a–e) indicate significant differences from monthly climatologies of each respective month at a 90% confidence level according to the Student's *t* test. Yellow shading in panels (a–e) indicates the period from January to May 1995.

term. The highest (lowest) temperatures are observed in austral summer (winter) when the net surface heat fluxes warming the ocean's upper layer are strongest (weakest) (Figure 8f). In addition, the residual term is a cooling term throughout the year. Further, the mean horizontal advection plays a cooling role, especially during austral winter (Figure 8f), when the Angola-Benguela front is located furthest north. Still, the temperature gradient and currents are stronger in the meridional direction suggesting that the meridional advection plays a more prominent role in this term than the zonal. In fact, the October peak in warming due to advection (Figure 8f) is sustained by the southward Angola Current bringing warm equatorial waters further south (Körner et al., 2023).

Figure 8g depicts the anomalies of each term of the heat budget equation during the 1995 Benguela Niño, while Figures 8a–8e show anomalies significantly different in relation to the monthly climatology (i.e., black stars). During the event's development and demise significant shifts in the ML temperature for the coastal area were observed at its onset in February, at its peak in March 1995, and at its demise in May 1995 (Figure 8a). Within this period we can as well observe the reduced temperature gradient between the ML and its base (Figure 8e).

During February and March, for instance, the ML temperature gradient is almost 3 times weaker than climatologically. Hence, we focus on explaining the anomalies within these months (i.e., yellow shading in Figures 8a–8e). In February 1995, the advection term was the only contributor to the warming of the mixed layer off Angola, concomitant with the strong anomalous poleward surface current in this month (Figure 5c), bringing warm waters further south. Even though the net heat flux average for the coastal box 1 indicates a net cooling during this month (Figure 8g), from the spatial anomalies (Figure S8b in Supporting Information S1) we can see a positive anomaly from 8°S to 13°S, which might also have contributed to warming the waters further advected southward. In addition, positive residual anomalies are present at the coast during February (Figure S8d in Supporting Information S1), from the River mouth until 15°S. The net residual cooling in February appears to be counteracting the advection warming, although the residual shift in this month is not significant (Figure 8d). On the other hand, in March 1995 during the peak of the event, the advection term stood for only 8% of the sum of the anomalous warming terms at the coast off Angola (Figure 8g), contributing mostly to the warming offshore of the box (Figure S8c in Supporting Information S1). The main contributor to warming up the mixed layer at the coastal region in March was by far the residual term (i.e., 92%, Figure 8g). Noteworthy, the residual spatial positive anomalies during March agree well with the SSS and BLT anomalies up to 18°S (Figure S8 in Supporting Information S1 and Figures 2b and 2c). The same is observed for the following April. The significantly reduced ML temperature gradient within these months indicates the location of the mixed layer base within the isothermal layer (Figures 1b and 1c), which leads to reduced turbulent heat loss at the base of the ML, since the turbulent mixing acts on a weak vertical temperature gradient (White & Toumi, 2014). Consequently, strong positive residual anomalies are observed in March and April. In fact, turbulent heat loss, here included in the residual term, is a crucial mechanism in this region not only for the cooling especially near the coast but also for an upward salt flux, bringing the more saline subsurface water toward the surface (Awo et al., 2022; Körner et al., 2023). The high residual anomaly maintained the surface warming during March 1995, countering the surface cooling in the same month due to surface heat fluxes. This damping term in the heat fluxes was mainly due to a significant latent heat loss in March 1995 (Figure S6 in Supporting Information S1). In April 1995 the high positive anomaly in the residual term (i.e., possibly related to the remaining stability due to the lower surface salinity during this month) was counteracted by surface heat fluxes and the northward advection of cool waters from the south, which contributed to the demise the event. The residual term will also be discussed in the next section.

Overall, when considering the mean interannual anomalies for each term (Figure S7 in Supporting Information S1) we find that the 1995 Benguela Niño event stands out especially in terms of advection, residual, and ML temperature gradient anomalies. The advection anomaly in February 1995 was in fact the highest positive advection anomaly observed in the 27 years analyzed period (Figure S7a in Supporting Information S1). The advection term has acted as the main factor to initially warm the surface waters by bringing warmer equatorial waters to the ABA. The extremely strong poleward current might also have contributed to taking this warming further south than 20°S. At the same time, one of the strongest residual anomalies was also seen during the 1995 event, together with the most negative anomaly in the ML temperature gradient for almost three decades (Figures S7d–S7e in Supporting Information S1). In fact, Figure S7e in Supporting Information S1 shows that this gradient was also extremely reduced during the 2016 warming event, which was also likely to have been influenced by an anomalous freshwater input (Lübbecke et al., 2019). Indeed, the ML temperature gradient anomaly time-series agrees quite well with both the N^2 and BLT anomaly time-series (i.e., r = −0.41, r = −0.53, respectively) as well as with the SSS anomalies (i.e., r = 0.48). Finally, the increased southward advection and reduced temperature vertical gradient might likewise have been impacted by the passage of a CTW (Sea Level Anomaly (SLA) in Figure 8e). Hence, our results suggest that the combination of the initial strong advection by the poleward current at the surface, and subsequently less turbulent mixing due to higher water column stability resulted in the strongest Benguela Niño event ever recorded in the satellite era.

4. Summary and Discussion

In this study, we described the strong 1995 Benguela Niño and investigated the role of anomalous freshwater input into the ABA (8°S–20°S, 8°E to the coast) during this event. We analyzed the impact of this low-salinity anomaly on the temperature change within the mixed layer at the onset of the warming, highlighting the importance of the dynamical mechanism that allowed the freshwater plume to be advected from north of Angola to the ABA.

The 1995 Benguela Niño developed in February 1995 and peaked in the following March with averaged SST anomalies of up to 2.5°C in the ABA coastal region (8°S–20°S, 1° away from the coast). Simultaneously, an anomalous low-salinity plume was present in the region, shoaling the mixed layer and generating higher water column stratification and stability due to barrier layer anomalies of up to 15 m. A large barrier layer contributes to the surface warming by inhibiting the cooling from below due to entrainment and mixing. The strong freshwater input resulted from a combination of the anomalous high CRD and precipitation in the months prior to the event and was advected from around 2°–5°S to 18°S, much further south than climatologically expected (Awo et al., 2022). This low-salinity plume advection was only possible due to a concomitant surfacing and strengthening of the Angola Current, which occurred due to a weakening of the coastal wind stress curl and wind stress during the event, allowing the current core to be present at the coast and to move from subsurface to the surface. This anomalous poleward transport partially explaining the intensity of the 1995 event was also suggested by Rouault (2012).

In addition to this, a CTW might also have played a role in strengthening the southward current. A previous study recorded the presence of an intraseasonal downwelling CTW in March 1995, 2 weeks before the peak of the event, with an amplitude of almost 3 cm (Imbol Koungue & Brandt, 2021). Furthermore, a much higher than usual Angola Current transport of 11 Sv from January–March 1995 was reported during the 1995 Benguela Niño (Mercier et al., 2003). Moreover, Sena Martins and Stammer (2022) recently stated that the causes of low-salinity anomalies spreading southward in this area were a higher CRD combined with the occurrence of the CTW between February and March. Hence, since the Angola Current variability is highly controlled by the passage of these waves (Bachèlery et al., 2016b; Kopte et al., 2017; Tchipalanga, Dengler, et al., 2018), we suggest that this CTW might also have contributed to the strong southward current transport. It appears that during the 1995 event, the combination of relaxed southerly winds offshore and the weakening of the wind stress curl at the coast, uplifting the Angola Current core to the surface, with the apparent presence of the CTW and an above climatology freshwater input in the region were the mechanisms that allowed low-salinity anomalies to reach the ABA.

The mixed layer heat budget analysis approach has been widely used to identify sources of surface warming in the tropical Atlantic, both from observational data sets (e.g., Foltz et al., 2003, 2020; Hummels et al., 2014; Hummels et al., 2020; Körner et al., 2023), and reanalysis product (Ma et al., 2023). Our analysis showed that anomalous advection was responsible for the warming at the onset of the event, in February, while the residual term was the main contributor during the peak of the event in March. In this study, the residual term includes the effect of turbulent mixing, processes not represented by the temporal and spatial scale of the data set here used, and errors of the other terms. The errors in this region are likely influenced by uncertainties arising from the SWR in the net surface heat fluxes (Körner et al., 2023) due to poor representation of shallow clouds (Huang et al., 2007). Additionally, sub-monthly variability within the Angolan coast (Bachèlery et al., 2016b; Goubanova et al., 2013) is likely to contribute to the residual term. However, the residual of the ML heat budget in this region can be assumed to be largely explained by the turbulent mixing at the base of the ML, especially in shallow regions close to the coast (Körner et al., 2023). The energy source of the turbulent mixing is the interaction of internal waves with the continental slope (Zeng et al., 2021). Zeng et al. (2021) find that the mixing is essentially more effective when stratification is weaker. The stratification in the ABA region is connected to freshwater fluxes, surface heat fluxes, and the passage of CTWs (Awo et al., 2022; Körner et al., 2023; Zeng et al., 2021). The freshwater plume present in coastal waters during the 1995 Benguela Niño influences turbulent mixing at the base of the mixed layer in two ways. Firstly, the available energy for mixing acts on a stronger stratification decreasing the eddy diffusivity (Körner et al., 2023; White & Toumi, 2014; Zeng et al., 2021). Secondly, in the presence of high freshwater input and the consequent barrier layer formation, the temperature gradient between the mixed layer and the water below it (i.e., $\overline{T}_{ML} - T_{-h}$) is close to zero (e.g., Echols & Riser, 2020), as the mixed layer base resides within the isothermal layer. Thus, the turbulent mixing acts on a weak vertical temperature gradient (White & Toumi, 2014). Hence, the anomalously high freshwater during early 1995 reduces the turbulent heat loss. The barrier layer presence and higher water column stability impact were observed especially in March 1995. It is also likely that this impact remained important in April 1995 since an anomaly in the residual term was still high in this month. Overall, we showed that an anomalous freshwater input in the ABA can indeed significantly contribute to the surface warming during a Benguela Niño, and should also be taken into account as a local forcing for these events. We also observed that this influence strongly depends on the advection of the freshwater to the south and thus on shifts in the wind field.

The influence of freshwater input in the generation of barrier layers in the southeastern tropical Atlantic that increased ocean stratification and stability has been discussed in previous studies (Lübbecke et al., 2019; Materia et al., 2012; Sena Martins & Stammer, 2022; White & Toumi, 2014). Salinity shifts impacting surface warming

in the tropical Atlantic via barrier layer formation and stratification have also been recently assessed (Gévaudan et al., 2021). There is, however, no consensus on the importance of barrier layers generating surface warming in the Equatorial and tropical Atlantic. While Pailler et al. (1999) and Foltz and McPhaden (2009) indicated strong warming related to barrier layers, Balaguru et al. (2012), Hernandez et al. (2016), and Gévaudan et al. (2021) found no significant relationship between these variables based on models. It was seen that salinity stratification can indeed play a major role in stabilizing surface layers of the ocean, leading to the upper-layer warming (Maes & O'Kane, 2014). However, it is hard to establish a direct correlation on interannual timescales also for the southeastern tropical Atlantic (Sena Martins & Stammer, 2022; White & Toumi, 2014), due to different processes affecting and changing the SST. When referring to Benguela Niños, it seems even more difficult, since the freshwater input does not seem to trigger these events, which are caused either remotely by the propagation of an equatorial Kelvin wave followed by a CTW at the African coast due to equatorial wind shifts, or by local atmospheric and wind changes (Florenchie et al., 2004; Imbol Koungue et al., 2019; Richter et al., 2010; Rouault et al., 2018). Still, such unique freshwater propagation as in this specific 1995 event indeed contributed to the surface warming.

In relation to Benguela Niñas, we believe that a lower freshwater input would not be an important factor in intensifying these cooling events. Climatologically, the low salinity plume is not usually spread over the whole ABA (Awo et al., 2022). Hence, in anomalous years of lower precipitation/river discharge, no significant change in the stratification off Angola would be observed. High freshwater input could, however, be a factor counteracting a cooling event. In these cases, the SST change during a Benguela Niña would be decreased, since the cooling event would be counteracted by the warming due to lower SSS and higher stratification. Still, this is very speculative and overall we believe that a freshwater input would not impact a Benguela Niña event the same way as it could do with the Benguela Niños.

Some open questions remain and should be approached in future studies. First, it is still unclear which mechanism is the most prominent driver in generating the negative salinity anomalies in ABA. We wonder if a high anomalous freshwater input would be enough to generate such anomalies, or if this freshwater plume presence in the Angolan-Nambian coast is only possible combined with a stronger Angola Current core at the surface. It is likely that in years of strong poleward Angola Current, freshwater especially from the CRD might be brought to the ABA. However, is it uncertain if solely the freshwater transport could generate stratification anomalies or if an anomalous freshwater input is also required. Further, White and Toumi (2014) when evaluating the impact of the amount of freshwater input from the Congo River on the spatial distribution of SST, did not find any significant changes between the control and the double CRD simulations. They suggested that the location of temperature changes is more dependent on environmental conditions than on the magnitude of the freshwater input (White & Toumi, 2014). In addition, the most important freshwater source to generate such salinity anomalies could not be clearly distinguished in our study between an anomalous CRD or precipitation. Different model simulations and experiments with climatological and reference river runoff and precipitation, like the works from Zhang and Busalacchi (2009) and White and Toumi (2014) could provide these answers. Furthermore, besides the 1995 Benguela Niño and the 2016 warming event, we highlight that the freshwater might also impact other events (e.g., 2001 Benguela Niño) as shown by the time series anomalies in Figure 3. Thus, the general influence of the freshwater input on the SST variability in the southeastern tropical Atlantic is still not well defined. Still, we could conclude from the present analysis that the freshwater input into the ABA related to the strength of the Angola Current is an active local forcing player in the intensification of Benguela Niños.

Conflict of Interest

The authors declare no conflicts of interest relevant to this study.

Data Availability Statement

All data sets and products used in this work are freely available in the following links: OISST (https://psl.noaa.gov/data/gridded/data.noaa.oisst.v2.highres.html); CCMP 6-hourly wind vectors (https://www.remss.com/measurements/ccmp/); ECMWF ERA5 surface heat flux (https://cds.climate.copernicus.eu/cdsapp#!/dataset/reanalysis-era5-single-levels-monthly-means?tab=form); The near-surface drifter-wind-altimetry synthesis can be accessed via: (https://www.aoml.noaa.gov/ftp/phod/pub/lumpkin/decomp/); Congo River discharge was obtained from (https://hybam.obs-mip.fr/data/); Precipitation from the GPCP product is available via (https://psl.noaa.gov/

data/gridded/data.gpcp.html); GLORYS12 product is available at (https://data.marine.copernicus.eu/product/GLOBAL_MULTIYEAR_PHY_001_030/download); CTD profiles from the Nansen Programme are publicly available at https://doi.pangaea.de/10.1594/PANGAEA.886492 (Tchipalanga, Ostrowski, & Dengler, 2018). Flow velocities from mooring data at 11°S are available at https://doi.pangaea.de/10.1594/PANGAEA.939249 (Hummels et al., 2021). CTD sections from previous cruises can be accessed via: M98 (2013; https://doi.pangaea.de/10.1594/PANGAEA.868640), Krahmann & Brandt, 2016); M120 (2015; https://doi.pangaea.de/10.1594/PANGAEA.868654, Kopte & Dengler, 2016); M131 (2016; https://doi.pangaea.de/10.1594/PANGAEA.910994, Brandt et al., 2020); M148 (2018; https://doi.pangaea.de/10.1594/PANGAEA.928997, Dengler et al., 2021); M158 (2019; https://doi.org/10.1594/PANGAEA.952354, Brandt et al., 2022).

References

Adler, R. F., Huffman, G. J., Chang, A., Ferraro, R., Xie, P.-P., Janowiak, J., et al. (2003). The version-2 global precipitation climatology project (GPCP) monthly precipitation analysis (1979–present). *Journal of Hydrometeorology*, 4(6), 1147–1167. https://doi.org/10.1175/1525-7541(2003)004%3C1147:TVGPCP%3E2.0.CO;2

Atlas, R., Hoffman, R. N., Ardizzone, J., Leidner, S. M., Jusem, J. C., Smith, D. K., & Gombos, D. (2011). A cross-calibrated, multiplatform ocean surface wind velocity product for meteorological and oceanographic applications. *Bulletin America Meteorology Social*, 92(2), 157–174. https://doi.org/10.1175/2010BAMS2946.1

Awo, F. M., Rouault, M., Ostrowski, M., Tomety, F. S., Da-Allada, C. Y., & Jouanno, J. (2022). Seasonal cycle of sea surface salinity in the Angola upwelling system. *Journal of Geophysical Research: Oceans*, 127(7), e2022JC018518. https://doi.org/10.1029/2022JC018518

Bachèlery, M.-L., Illig, S., & Dadou, I. (2016). Forcings of nutrient, oxygen, and primary production interannual variability in the southeast Atlantic Ocean. *Geophysical Research Letters*, 43(16), 8617–8625. https://doi.org/10.1002/2016GL070288

Bachèlery, M. L., Illig, S., & Dadou, I. (2016). Interannual variability in the South-East Atlantic Ocean, focusing on the Benguela upwelling system: Remote versus local forcing. *Journal of Geophysical Research: Oceans*, 121(1), 284–310. https://doi.org/10.1002/2015JC011168

Bachèlery, M. L., Illig, S., & Rouault, M. (2020). Interannual coastal trapped waves in the Angola-Benguela upwelling system and Benguela Niño and Niña events. *Journal of Marine Systems*, 203, 103262. https://doi.org/10.1016/j.jmarsys.2019.103262

Balaguru, K., Chang, P., Saravanan, R., & Jang, C. J. (2012). The barrier layer of the Atlantic warmpool: Formation mechanism and infuence on the mean climate. *Tellus A: Dynamic Meteorology and Oceanography*, 64(1), 18162. https://doi.org/10.3402/tellusa.v64i0.18162

Binet, D., Gobert, B., & Maloueki, L. (2001). El Niño-like warm events in the Eastern Atlantic (6°N and 20°S) and fish availability from Congo to Angola (1964–1999). *Aquatic Living Resources*, 14(2), 99–113. https://doi.org/10.1016/S0990-7440(01)01105-6

Blamey, L. K., Shannon, L. J., Bolton, J. J., Crawford, R. J. M., Dufois, F., Evers-King, H., et al. (2015). Ecosystem change in the southern Benguela and the underlying processes. *Journal of Marine Systems*, 144, 9–29. https://doi.org/10.1016/j.jmarsys.2014.11.006

Boyer, D. C., & Hampton, I. (2001). An overview of the living marine resources of Namibia. *South African Journal of Marine Science*, 23(1), 5–35. https://doi.org/10.2989/025776101784528953

Brandt, P., Alory, G., Awo, F. M., Dengler, M., Djakouré, S., Imbol Koungue, R. A., et al. (2023). Physical processes and biological productivity in the upwelling regions of the tropical Atlantic. *Ocean Science*, 19(3), 581–601. https://doi.org/10.5194/os-19-581-2023

Brandt, P., Kopte, R., & Krahmann, G. (2020). Physical oceanography (CTD) during METEOR cruise M131. PANGAEA. [Dataset]. https://doi.org/10.1594/PANGAEA.910994

Brandt, P., Subramaniam, A., Schmidtko, S., & Krahmann, G. (2022). Physical oceanography (CTD) during METEOR cruise M158. PANGAEA. [Dataset]. https://doi.org/10.1594/PANGAEA.952354

de Boyer Montégut, C., Madec, G., Fischer, A. S., Lazar, A., & Iudicone, D. (2004). Mixed layer depth over the global ocean: An examination of profile data and a profile-based climatology. *Journal of Geophysical Research*, 109(C12). https://doi.org/10.1029/2004JC002378

de Boyer Montégut, C., Mignot, J., Lazar, A., & Cravatte, S. (2007). Control of salinity on the mixed layer depth in the world ocean: 1. General description. *Journal of Geophysical Research*, 112(C6). https://doi.org/10.1029/2006JC003953

Dengler, M., Brandt, P., Herrford, J., & Krahmann, G. (2021). Physical oceanography (CTD) during METEOR cruise M148. PANGAEA. [Dataset]. https://doi.org/10.1594/PANGAEA.928997

Echols, R., & Riser, S. C. (2020). The impact of barrier layers on Arabian Sea surface temperature variability. *Geophysical Research Letters*, 47(3), e2019GL085290. https://doi.org/10.1029/2019GL085290

Fennel, W., Junker, T., Schmidt, M., & Mohrholz, V. (2012). Response of the Benguela upwelling systems to spatial variations in the wind stress. *Continental Shelf Research*, 45, 65–77. https://doi.org/10.1016/j.csr.2012.06.004

Florenchie, P., Reason, C. J. C., Lutjeharms, J. R. E., Rouault, M., Roy, C., & Masson, S. (2004). Evolution of interannual warm and cold events in the southeast Atlantic Ocean. *Journal of Climate*, 17(12), 2318–2334. https://doi.org/10.1175/1520-0442(2004)017<2318:eoiwac>2.0.co;2

Foltz, G. R., Grodsky, S. A., Carton, J. A., & McPhaden, M. J. (2003). Seasonal mixed layer heat budget of the tropical Atlantic Ocean. *Journal of Geophysical Research*, 108(C5), 3146. https://doi.org/10.1029/2002jc001584

Foltz, G. R., Hummels, R., Dengler, M., Perez, R. C., & de Araujo, M. (2020). Vertical turbulent cooling of the mixed layer in the Atlantic ITCZ and trade wind regions. *Journal of Geophysical Research: Oceans*, 125(2), e2019JC015529. https://doi.org/10.1029/2019JC015529

Foltz, G. R., & McPhaden, M. J. (2009). Impact of barrier layer thickness on SST in the central tropical North Atlantic. *Journal of Climate*, 22(2), 285–299. https://doi.org/10.1175/2008JCLI2308.1

Gammelsrød, T., Bartholomae, C. H., Boyer, D. C., Filipe, V. L. L., & O'Toole, M. J. (1998). Intrusion of warm surface water along the Angolan-Namibian coast in February–March 1995: The 1995 Benguela Niño. *South African Journal of Marine Science*, 19(1), 41–56. https://doi.org/10.2989/025776198784126719

Gévaudan, M., Jouanno, J., Durand, F., Morvan, G., Renault, L., & Samson, G. (2021). Infuence of ocean salinity stratifcation on the tropical Atlantic Ocean surface. *Climate Dynamics*, 57(1–2), 321–340. https://doi.org/10.1007/s00382-021-05713-z

Goubanova, K., Illig, S., Machu, E., Garçon, V., & Dewitte, B. (2013). SST subseasonal variability in the central Benguela upwelling system as inferred from satellite observations (1999–2009). *Journal of Geophysical Research: Oceans*, 118(9), 4092–4110. https://doi.org/10.1002/jgrc.20287

Hansingo, K., & Reason, C. J. C. (2009). Modelling the atmospheric response over southern Africa to SST forcing in the southeast tropical Atlantic and southwest subtropical Indian Oceans. *International Journal of Climatology*, 29(7), 1001–1012. https://doi.org/10.1002/joc.1919

Hernandez, O., Jouanno, J., & Durand, F. (2016). Do the Amazon and Orinoco freshwater plumes really matter for hurricane-induced ocean surface cooling? *Journal of Geophysical Research: Oceans*, *121*(4), 2119–2141. https://doi.org/10.1002/2015JC011021

Hersbach, H., Bell, B., Berrisford, P., Hirahara, S., Horányi, A., Muñoz-Sabater, J., et al. (2020). The ERA5 global reanalysis. *Quarterly Journal of the Royal Meteorological Society*, *146*(730), 1999–2049. https://doi.org/10.1002/qj.3803

Hu, Z., & Huang, B. (2007). Physical processes associated with the tropical Atlantic SST gradient during the anomalous evolution in the southeastern ocean. *Journal of Climate*, *20*(14), 3366–3378. https://doi.org/10.1175/JCLI4189.1

Huang, B., Hu, Z. Z., & Jha, B. (2007). Evolution of model systematic errors in the tropical Atlantic basin from coupled climate hindcasts. *Climate Dynamics*, *28*(7–8), 661–682. https://doi.org/10.1007/s00382-006-0223-8

Huang, B., Liu, C., Banzon, V., Freeman, E., Graham, G., Hankins, B., et al. (2021). Improvements of the daily Optimum interpolation sea surface temperature (DOISST) version 2.1. *Journal of Climate*, *34*(8), 2923–2939. https://doi.org/10.1175/JCLI-D-20-0166.1

Hummels, R., Dengler, M., Brandt, P., & Schlundt, M. (2014). Diapycnal heat flux and mixed layer heat budget within the Atlantic Cold Tongue. *Climate Dynamics*, *43*(11), 3179–3199. https://doi.org/10.1007/s00382-014-2339-6

Hummels, R., Dengler, M., Rath, W., Foltz, G., Schütte, F., Fischer, T., & Brandt, P. (2020). Surface cooling caused by rare but intense near-inertial wave induced mixing in the tropical Atlantic. *Nature Communications*, *11*(1), 3829. https://doi.org/10.1038/s41467-020-17601-x

Hummels, R., Imbol Koungue, R. A., Brandt, P., & Krahmann, G. (2021). Physical oceanography from mooring KPO_1215. PANGAEA. [Dataset]. https://doi.org/10.1594/PANGAEA.939249

Illig, S., Bachèlery, M.-L., & Lübbecke, J. F. (2020). Why do Benguela Niños lead Atlantic Niños? *Journal of Geophysical Research: Oceans*, *125*(9), e2019JC016003. https://doi.org/10.1029/2019JC016003

Imbol Koungue, R. A., & Brandt, P. (2021). Impact of intraseasonal waves on Angolan warm and cold events. *Journal of Geophysical Research: Oceans*, *126*(4), e2020JC017088. https://doi.org/10.1029/2020JC017088

Imbol Koungue, R. A., Brandt, P., Lübbecke, J., Prigent, A., Martins, M. S., & Rodrigues, R. R. (2021). The 2019 Benguela Niño. *Frontiers in Marine Science*, *8*, 800103. https://doi.org/10.3389/fmars.2021.800103

Imbol Koungue, R. A., Illig, S., & Rouault, M. (2017). Role of interannual Kelvin wave propagations in the equatorial Atlantic on the Angola Benguela Current system. *Journal of Geophysical Research: Oceans*, *122*(6), 4685–4703. https://doi.org/10.1002/2016JC012463

Imbol Koungue, R. A., Rouault, M., Illig, S., Brandt, P., & Jouanno, J. (2019). Benguela Niños and Benguela Niñas in forced ocean simulation from 1958 to 2015. *Journal of Geophysical Research: Oceans*, *124*(8), 5923–5951. https://doi.org/10.1029/2019JC015013

Junker, T., Schmidt, M., & Mohrholz, V. (2015). The relation of wind stress curl and meridional transport in the Benguela upwelling system. *Journal of Marine Systems*, *143*, 1–6. https://doi.org/10.1016/j.jmarsys.2014.10.006

Kopte, R., Brandt, P., Dengler, M., Tchipalanga, P. C. M., Macueria, M., & Ostrowski, M. (2017). The Angola current: Flow and hydrographic characteristics as observed at 11°S. *Journal of Geophysical Research: Oceans*, *122*(2), 1177–1189. https://doi.org/10.1002/2016JC012374

Kopte, R., & Dengler, M. (2016). Physical oceanography during METEOR cruise M120. PANGAEA. [Dataset]. https://doi.org/10.1594/PANGAEA.868654

Körner, M., Brandt, P., & Dengler, M. (2023). Seasonal cycle of sea surface temperature in the tropical Angolan Upwelling System. *Ocean Science*, *19*(1), 121–139. https://doi.org/10.5194/os-19-121-2023

Krahmann, G., & Brandt, P. (2016). Physical oceanography during METEOR cruise M98. PANGAEA. [Dataset]. https://doi.org/10.1594/PANGAEA.868640

Lellouche, J.-M., Greiner, E., Bourdallé Badie, R., Garric, G., Melet, A., Drévillon, M., et al. (2021). The copernicus global 1/12 oceanic and sea ice GLORYS12 reanalysis. *Frontiers in Earth Science*, *9*, 1–27. https://doi.org/10.3389/feart.2021.698876

Lübbecke, J. F., Böning, C. W., Keenlyside, N. S., & Xie, S. P. (2010). On the connection between Benguela and equatorial Atlantic Niños and the role of the South Atlantic Anticyclone. *Journal of Geophysical Research*, *115*(C9), C09015. https://doi.org/10.1029/2009JC005964

Lübbecke, J. F., Brandt, P., Dengler, M., Kopte, R., Lüdke, J., Richter, I., et al. (2019). Causes and evolution of the southeastern tropical Atlantic warm event in early 2016. *Climate Dynamics*, *53*(1–2), 261–274. https://doi.org/10.1007/s00382-018-4582-8

Lutz, K., Jacobeit, J., & Rathmann, J. (2015). Atlantic warm and cold water events and impact on African west coast precipitation. *International Journal of Climatology*, *35*, 128–141. https://doi.org/10.1002/joc3969

Ma, X., Liu, H., & Wang, X. (2023). Interannual variability of barrier layer in the tropical Atlantic and its relationship with the tropical Atlantic modes. *Journal of Physical Oceanography*, *53*(2), 573–594. https://doi.org/10.1175/JPO-D-21-0235.1

Maes, C., & O'Kane, T. J. (2014). Seasonal variations of the upper ocean salinity stratification in the tropics. *Journal of Geophysical Research: Oceans*, *119*(3), 1706–1722. https://doi.org/10.1002/2013JC009366

Materia, S., Gualdi, S., Navarra, A., & Terray, L. (2012). The effect of Congo River freshwater discharge on eastern equatorial Atlantic climate variability. *Climate Dynamics*, *39*(9–10), 2109–2125. https://doi.org/10.1007/s00382-012-1514-x

Mears, C., Lee, T., Ricciardulli, L., Wang, X., & Wentz, F. (2022). Improving the accuracy of the cross-calibrated multi-platform (CCMP) ocean vector winds. *Remote Sensing*, *14*(17), 4230. https://doi.org/10.3390/rs14174230

Mercier, H., Arhan, M., & Lutjeharms, J. R. E. (2003). Upper-layer circulation in the eastern equatorial and South Atlantic ocean in January–March 1995. *Deep-Sea Research I*, *50*(7), 863–887. https://doi.org/10.1016/S0967-0637(03)00071-2

Mignot, J., Lazar, A., & Lacarra, M. (2012). On the formation of barrier layers and associated vertical temperature inversions: A focus on the northwestern tropical Atlantic. *Journal of Geophysical Research*, *117*(C2). https://doi.org/10.1029/2011JC007435

Moisan, J. R., & Niiler, P. P. (1998). The seasonal heat budget of the North Pacific: Net heat flux and heat storage rates (1950–1990). *Journal of Physical Oceanography*, *28*, 401–421. https://doi.org/10.1175/1520-0485(1998)028<0401:TSHBOT>2.0.CO;2

Pailler, K., Bourlès, B., & Gouriou, Y. (1999). The barrier layer in the western tropical Atlantic Ocean. *Geophysical Research Letters*, *26*(14), 2069–2072. https://doi.org/10.1029/1999GL900492

Patricola, M. C., & Chang, P. (2017). Structure and dynamics of the Benguela low-level coastal jet. *Climate Dynamics*, *49*(7–8), 2765–2788. https://doi.org/10.1007/s00382-016-3479-7

Polo, I., Lazar, A., Rodriguez-Fonseca, B., & Arnault, S. (2008). Oceanic Kelvin waves and tropical Atlantic intraseasonal variability: 1. Kelvin wave characterization. *Journal of Geophysical Research*, *113*, C07009. https://doi.org/10.1029/2007JC004495

Reynolds, R. W., Smith, T. M., Liu, C., Chelton, D. B., Casey, K. S., & Schlax, M. G. (2007). Daily high-resolution-blended analyses for sea surface temperature. *Journal of Climate*, *20*(22), 5473–5496. https://doi.org/10.1175/2007jcli1824.1

Richter, I., Behera, S. K., Masumoto, Y., Taguchi, B., Komori, N., & Yamagata, T. (2010). On the triggering of Benguela Niños: Remote equatorial versus local influences. *Geophysical Research Letters*, *37*(20), L20604. https://doi.org/10.1029/2010GL0444461

Rouault, M. (2012). Bi-annual intrusion of tropical water in the northern Benguela upwelling. *Geophysical Research Letters*, *39*(12), L12606. https://doi.org/10.1029/2012GL052099

Rouault, M., Florenchie, P., Fauchereau, N., & Reason, C. J. C. (2003). South East tropical Atlantic warm events and southern African rainfall. *Geophysical Research Letters*, *30*(5), 8009. https://doi.org/10.1029/2003GL014840

Rouault, M., Illig, S., Lübbecke, J., & Koungue, R. A. I. (2018). Origin, development and demise of the 2010–2011 Benguela Niño. *Journal of Marine Systems*, *188*, 39–48. https://doi.org/10.1016/j.jmarsys.2017.07.007

Saha, A., Serra, N., & Stammer, D. (2021). Growth and decay of northwestern tropical Atlantic barrier layers. *Journal of Geophysical Research: Oceans*, *126*(5), e2020JC016956. https://doi.org/10.1029/2020JC016956

Sena Martins, M., & Stammer, D. (2022). Interannual variability of the Congo river plume-induced sea surface salinity. *Remote Sensing*, *14*(4), 1013. https://doi.org/10.3390/rs14041013

Shannon, L. V., Boyd, A. J., Brundrit, G. B., & Taunton-Clark, J. (1986). On the existence of an El Niño-type phenomenon in the Benguela system. *Journal of Marine Research*, *44*(3), 495–520. https://doi.org/10.1357/002224086788403105

Song, Q., Aiki, H., & Tang, Y. (2023). The role of equatorially forced waves in triggering Benguela Niño/Niña as investigated by an energy flux diagnosis. *Journal of Geophysical Research: Oceans*, *128*(4), e2022JC019272. https://doi.org/10.1029/2022JC019272

Stevenson, J. W., & Niiler, P. P. (1983). Upper Ocean heat budget during the Hawaii-to-Tahiti Schuttle experiment. *Journal of Physical Oceanography*, *13*(10), 1894–1907. https://doi.org/10.1175/1520-0485(1983)013<1894:uohbdt>2.0.co;2

Tchipalanga, P., Dengler, M., Brandt, P., Kopte, R., Macuéria, M., Coelho, P., et al. (2018). Eastern boundary circulation and hydrography off Angola: Building Angolan oceanographic capacities. *Bulletin of the American Meteorological Society*, *99*(8), 1589–1605. https://doi.org/10.1175/BAMS-D-17-0197.1

Tchipalanga, P., Ostrowski, M., & Dengler, M. (2018). Physical oceanography on the Angolan continental shelf and Cabinda. PANGAEA. [Dataset]. https://doi.org/10.1594/PANGAEA.886492

Vialard, J., & Delecluse, P. (1998). An OGCM study for the TOGA decade. Part I: Role of salinity in the physics of the western Pacific fresh pool. *Journal of Physical Oceanography*, *28*, 1071–1088. https://doi.org/10.1175/1520-0485(1998)028<1071:AOSFTT>2.0.CO;2

White, R. H., & Toumi, R. (2014). River flow and ocean temperatures: The Congo river. *Journal of Geophysical Research: Oceans*, *119*(4), 2501–2517. https://doi.org/10.1002/2014JC009836

Zeng, Z., Brandt, P., Lamb, K. G., Greatbatch, R. J., Dengler, M., Claus, M., & Chen, X. (2021). Three-dimensional numerical simulations of internal tides in the Angolan upwelling region. *Journal of Geophysical Research: Oceans*, *126*(2), e2020JC016460. https://doi.org/10.1029/2020JC016460

Zhang, R.-H., & Busalacchi, A. J. (2009). Freshwater flux (FWF)-Induced oceanic feedback in a hybrid coupled model of the tropical Pacific. *Journal of Climate*, *22*(4), 853–879. https://doi.org/10.1175/2008JCLI2543.1

References From the Supporting Information

Lumpkin, R., & Garzoli, S. L. (2011). Interannual to decadal changes in the western South Atlantic's surface circulation. *Journal of Geophysical Research*, *116*(C1), C01014. https://doi.org/10.1029/2010JC006285

Perez, R. C., Foltz, G. R., Lumpkin, R., & Schmid, C. (2019). Direct measurements of upper ocean horizontal velocity and vertical shear in the tropical North Atlantic at 4°N, 23°W. *Journal of Geophysical Research: Oceans*, *124*(6), 4133–4151. https://doi.org/10.1029/2019JC015064